

Counteranions and Solvent Influence CO₂ Reduction to Oxalate by Chalcogen-Bridged Tricopper Cyclophanates

Brian J. Cook,^{†,‡} Gianna N. Di Francesco,[†] Khalil A. Abboud,[†] and Leslie J. Murray^{*,†,‡,§}

[†]Center for Catalysis and [‡]Florida Center for Heterocyclic Compounds, Department of Chemistry, University of Florida, Gainesville, Florida 32611-7200, United States

S Supporting Information

ABSTRACT: One-electron reduction of Cu₃EL (L³⁻ = tris(β -diketiminate)cyclophane, and E = S, Se) affords [Cu₃EL]⁻, which reacts with CO₂ to yield exclusively C₂O₄²⁻ (95% yield, TON = 24) and regenerate Cu₃EL. Stopped-flow UV/visible data support an A→B mechanism under pseudo-first-order conditions ($k_{\text{obs}, 298\text{K}} = 115(2) \text{ s}^{-1}$), which is 10⁶ larger than those for reported copper complexes. The k_{obs} values are dependent on the counteranion and solvent (e.g., k_{obs} is greater for [K(18-crown-6)]⁺ vs (Ph₃P)₂N⁺, and there is a 20-fold decrease in k_{obs} in THF vs DMF). Our results suggest a mechanism in which cations and solvent influence the stability of the transition state.

There is an urgent need to utilize or trap CO₂ to mitigate climate change.¹ Although biological systems effectively fix CO₂ in photosynthesis,² similar chemical approaches remain limited and typically rely on activated nucleophiles or electrophiles.³ Conversion of CO₂ into reduced C₁ products (e.g., CO or HCOO⁻) electrochemically or with dihydrogen has been well explored.⁴ In contrast, homogeneous catalysts that facilitate C–C bond formation from CO₂ are scarce. CO₂ reduction products with C_{*n*}, where *n* ≥ 2, are observed in heterogeneous systems but are usually minor components.⁵ The simplest C–C coupled product from CO₂ reduction is oxalate, formally arising from one-electron reduction of two CO₂ molecules, followed by radical coupling.⁶ Few homogeneous systems catalyze CO₂ reduction to oxalate, or CO₂-RedOx (Figure 1).⁷ Jäger's electrocatalysts are proposed to liberate CO₂^{•-} from a transient Ni^I-CO₂, with radical coupling leading to oxalate.^{7b,8} Tanaka's [M₃S₂]²⁺ catalysts (M = Co, Rh, Ir) span a range of onset potentials with strong selectivity for oxalate formation but are hampered by slow reaction kinetics.^{7d} In Bouwman's electrocatalytic system, a dicopper(I) complex reacts with CO₂ in air to yield a bis[(μ -oxalato)dicopper(II)] product and requires Li⁺ to induce oxalate dissociation under catalytic turnover.^{7a} Relatedly, Maverick's dicopper complex is capable of CO₂RedOx, albeit under stoichiometric conditions or as a batch-process catalyst.⁹ Oxalate dissociation kinetics remain a challenge for CO₂RedOx, and particularly for the reported copper systems. The effect of cations and other reaction parameters on CO₂RedOx are underexplored for homogeneous systems; recent reports have interrogated solvent and cation effects on CO₂ reduction to formate and CO, respectively.¹⁰ Herein, we report CO₂RedOx by anionic (μ_3 -

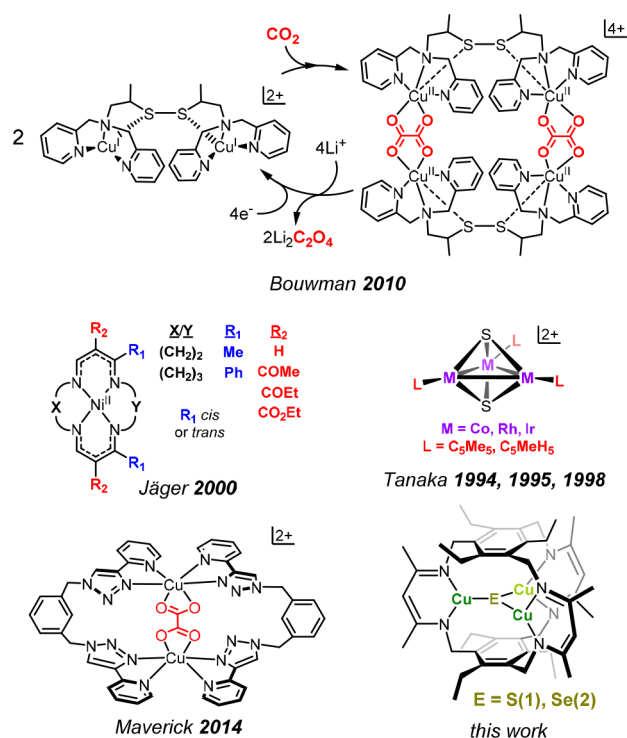


Figure 1. Reported catalysts for CO₂ reduction to C₂O₄²⁻. All except Maverick's are catalytic either chemically or under an applied potential.

sulfido)- and (μ_3 -selenido)tricopper complexes and the effect of the cation and solvent on CO₂RedOx rate.

Cu₃(μ_3 -S)L (1) and Cu₃(μ_3 -Se)L (2) can be readily reduced with 1.0 equiv of [K(18-crown-6)][C₁₀H₈] in THF to [K(18-crown-6)][1] and [K(18-crown-6)][2], as expected from the respective cyclic voltammograms (Figure S105).^{11–13} Notably, [K(18-crown-6)][1] and [K(18-crown-6)][2] are unreactive toward up to 5 equiv of H₂O, but react upon exposure to O₂. Although we were unable to obtain suitable single crystals of [K(18-crown-6)][Cu₃EL], we could readily crystallize reduction products of 1 and 2 using KC₁₀H₈, [K(THF)₃][1] and [K(THF)₃][2] are isostructural, with [K(THF)₃]⁺ interacting in an η^5 fashion with one β -diketiminate arm of a pseudo-D_{3h} [Cu₃EL]⁻ ion (Figures 2 and S104). Structures of 1⁻ and 2⁻ are also comparable to the parent neutral molecules with minor

Received: March 6, 2018

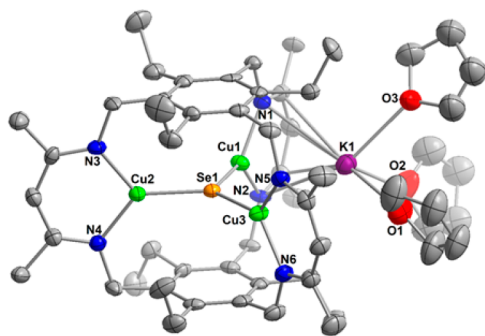


Figure 2. ORTEP representation (50% probability) of $[\text{K}(\text{THF})_3][\mathbf{2}]$. H-atoms and guest solvent are omitted for clarity. Cu, Se, C, N, and O atoms are depicted as lime green, orange, gray, blue, and red ellipsoids, respectively.

changes to the bond lengths.^{12,13} The structural changes observed upon reduction agree with the Cu–E π^* and Cu–N σ^* nature of the a_2'' LUMO of Cu_3EL reported elsewhere.^{12,13}

Exposure of thawing THF slurries of solid $[\text{K}(18\text{-crown-6})][\text{Cu}_3\text{EL}]$ to ~ 1 atm CO_2 results in dissolution of the -ate complexes to afford Cu_3EL in solution and a gray precipitate. This reaction takes ~ 30 min at -80 °C, with near-quantitative regeneration of Cu_3EL ($>99\%$ by mass), as confirmed by ^1H NMR spectra of product mixtures (Figures S37–S40). Resonances for free crown ether in these reactions are apparent in the spectra, suggesting dissociation of K^+ . The following data recorded on this precipitate support formation of an oxalate salt from CO_2 : (i) IR absorption bands range from 1615 to 1680 cm^{-1} (Figure S62); (ii) a single resonance is seen at ~ 160 ppm in ^{13}C NMR spectra (Figures S42 and S55); and (iii) the IR absorptions shift and the ^{13}C NMR resonance is enhanced in products from reaction using $^{13}\text{CO}_2$.^{7a,4,8,9} We conclude that $[\text{K}(18\text{-crown-6})][\text{Cu}_3\text{EL}]$ effects C–C coupling of CO_2 to yield $\text{K}_2\text{C}_2\text{O}_4$ and regenerate Cu_3EL . Importantly, the isolated yield for $\text{K}_2\text{C}_2\text{O}_4$ is 95%, exhibiting the high selectivity of the Cu_3EL complexes to effect CO_2RedOx .

As part of our prior report of **1**, we obtained preliminary data indicating no reactivity of $[\text{CoCp}^*_2][\mathbf{1}]$ toward CO_2 , strongly contrasting the observations for the $[\text{K}(18\text{-crown-6})]^+$ and $[\text{K}(\text{THF})_3]^+$ congeners.¹² We, therefore, synthesized compounds of the general formula $\text{Q}[\text{Cu}_3\text{EL}]$, where $\text{Q}^+ = \text{Ph}_4\text{P}^+$, PPN^+ ($\text{PPN}^+ = \text{bis}(\text{triphenylphosphine})\text{iminium}$), Bu_4N^+ , $[\text{FeCp}(\text{C}_6\text{Me}_6)]^+$, $[\text{K}(2.2.2\text{-cryptand})]^+$, $[\text{Na}(15\text{-crown-5})]^+$, and $[\text{Na}(\text{THF})_n]^+$, and evaluated reactions of these compounds with CO_2 . We followed reaction progress qualitatively by the diagnostic color change associated with regeneration of Cu_3EL , and analyzed product mixtures by ^1H NMR spectroscopy (Table S1). A cation dependence is evident from these data; complexes with alkali counteranions react at significantly lower temperatures than the organic cation congeners. Encapsulation of K^+ within 2.2.2-cryptand agrees with this trend. Additionally, $\mathbf{2}^-$ is more reactive toward CO_2 than $\mathbf{1}^-$, consistent with $\mathbf{2}^-$ having a ~ 3.5 kcal/mol greater driving force given that $E_{1/2}(\mathbf{2}) - E_{1/2}(\mathbf{1}) = -0.15$ V (Figure S105).^{12,13} As for reactions with $[\text{K}(18\text{-crown-6})][\text{Cu}_3\text{EL}]$, free crown ether or cryptand is observed in ^1H NMR spectra of products from reaction of, respectively, $[\text{Na}(15\text{-crown-5})]^+$ or $[\text{K}(2.2.2\text{-cryptand})]^+$ salts with CO_2 (Figures S46 and S47).

Given that **1** and **2** are regenerated, we postulated that these complexes could function as homogeneous catalysts, and evaluated the reaction products of CO_2 with either CoCp^*_2

($E_{1/2} = -1.94$ V vs Fc/Fc^+), $\text{FeCp}(\text{C}_6\text{Me}_6)$ ($E_{1/2} = -2.07$ V), or KC_8 ($E_{1/2} < -3.7$ V)¹⁴ in the presence or absence of 2 mol% Cu_3EL . For the CoCp^*_2 reaction, $[\text{CoCp}^*_2][\text{Cu}_3\text{EL}]$ and CoCp^*_2 are recovered; inclusion of stoichiometric KPF_6 relative to CoCp^*_2 in the reaction results in consumption of the reductant and formation of $\text{K}_2\text{C}_2\text{O}_4$. Similarly, catalysis is observed for $\text{FeCp}(\text{C}_6\text{Me}_6)$ only in the presence of KPF_6 and for KC_8 (Figures S58–S60). The $\text{C}_2\text{O}_4^{2-}$ yield exceeds 95% ($\text{TON} = 24$) with respect to reductant using **2** as a catalyst, but is lower for **1** (54%).²⁵ Minimal oxalate is observed in the absence of **1** or **2** (Figures S59 and S60), independent of reductant. These results highlight the catalytic potential of **1** and **2** for CO_2RedOx and reinforce the observed cation influence.

To quantify the cation effect, we monitored single-turnover reactions of $\mathbf{1}^-$ and $\mathbf{2}^-$ with CO_2 by stopped-flow UV/visible spectrophotometry (Figure 3). DMF was our initial solvent choice because of concerns with oxalate precipitation (Figure S55).²⁴ Absorption data of the reaction of $[\text{K}(18\text{-crown-6})][\mathbf{1}]$ with CO_2 (168 equiv) in DMF at -55 °C evidence formation of **1**; thus, an A \rightarrow B mechanism was used to model all data sets, as no intermediates were detected. The estimated pseudo-first-

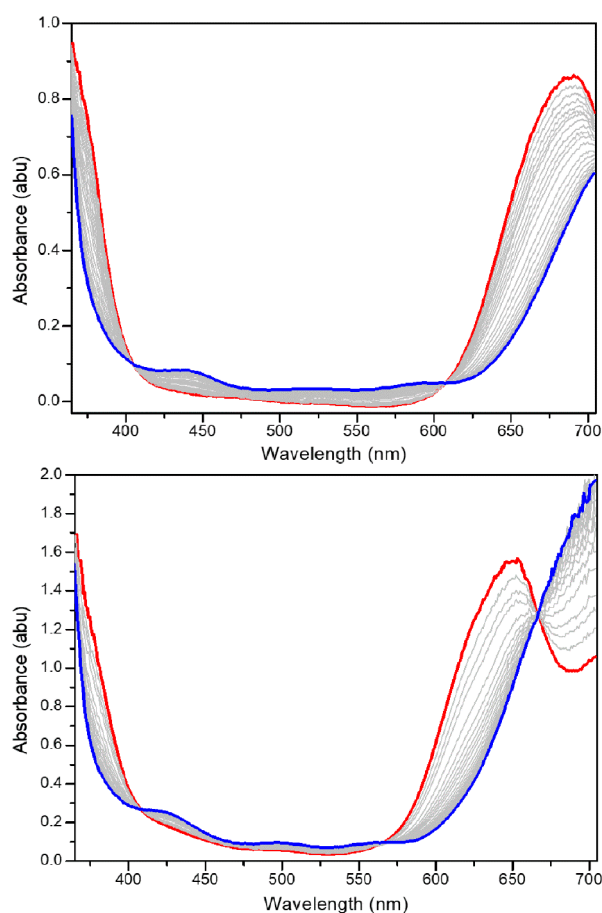


Figure 3. Stopped-flow UV/visible spectra in the 300–700 nm range recorded at -55 °C in DMF for reaction of 8.4 mM CO_2 with 0.05 mM $[\text{K}(18\text{-crown-6})][\mathbf{1}]$ (top) and 0.12 mM $[\text{K}(18\text{-crown-6})][\mathbf{2}]$ (bottom). Isosbestic points are observed at 406 and 608 nm (top) and at 408, 567, and 667 nm (bottom). Red trace represents the first time point at 2.5 ms, and blue trace represents the spectrum at 1500 ms. Relative to unreacted $[\text{K}(18\text{-crown-6})][\mathbf{2}]$, A_{645} decreases by ~ 0.40 within the instrument dead time.

Table 1. Values for k_{obs} and Calculated Activation Parameters for CO_2RedOx by I^-

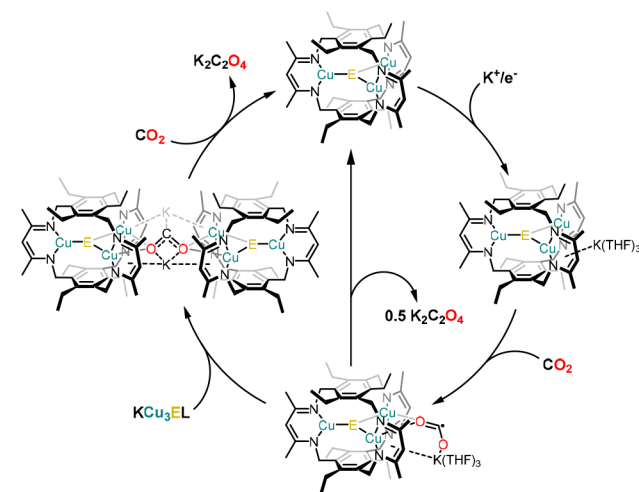
countercation	k_{obs} (s^{-1})			ΔH^\ddagger (kcal/mol)	ΔS^\ddagger (cal/mol·K)	ΔG^\ddagger_{298} (kcal/mol)
	-55 °C	-15 °C	25 °C ^c			
[K(18-crown-6)] ⁺ ^a	11(2)	49(1)	115(2)	2.9(1)	-39(1)	14.6(4)
[PPN] ⁺ ^a	6.3(5)	38(5)	141(9)	4.0(3)	-35(4)	15(1)
[PPN] ⁺ ^b	0.39(4)	0.93(3)	11(1)	5.0(3)	-37(5)	16(2)
[K(THF) ₃] ⁺ ^a	14(1)	>231 ^d	>231 ^d	1.85(0.24)	-44(16)	15(5)

^aSolvent = DMF. ^bSolvent = THF. ^c25 °C values extrapolated from Eyring–Polanyi analysis. ^d k_{obs} estimated based on 3 ms instrument dead time

order rate constant for reaction of [K(18-crown-6)][2] with CO_2 ($k_{\text{obs}} > 231 \text{ s}^{-1}$) is significantly greater than that for [K(18-crown-6)][1] ($k_{\text{obs}} = 11(2) \text{ s}^{-1}$), as 50+% of 2^- reacts within the 3 ms instrument dead time (Figure S65). All subsequent kinetic analyses were performed with I^- salts, as the reaction rate for 2^- precludes an accurate determination of k_{obs} . Kinetic data collected at λ_{max} of I^- (680 nm) and of **1** (805 nm) at various temperatures were reliably fit to a single exponential, affording statistically indistinguishable k_{obs} values (Figure S66–S102). Calculated activation parameters evidence a low ΔH^\ddagger and a large ΔS^\ddagger (Table 1) to afford ΔG^\ddagger_{298} values comparable to experimentally and computationally determined values for other CO_2RedOx reactions.¹⁵ Surprisingly, k_{obs} is either inverse first or second order in $[\text{CO}_2]$ (Table S4 and Figure S103), and implicates a more complex mechanism than generation and homocoupling of freely diffusing $\text{CO}_2^{\bullet-}$. Similar experiments performed using THF as the solvent instead of DMF revealed a significant solvent effect (Table 1 and Figures S92–S96). The solvent trend is consistent with the observed cation effect, providing two variables to tune the CO_2RedOx rate in this system.

Bouwman's and Maverick's compounds have slow rate constants for oxalate formation (4.76×10^{-4} and $5.28 \times 10^{-6} \text{ s}^{-1}$, respectively), and both require weak reductants to effect CO_2RedOx .^{7a,9,15b} In addition, product inhibition is likely a limiting step under turnover conditions for these systems. Similar product inhibition is inferred for the bis[β -diketiminatonickel(I)] complex from Limberg and co-workers.⁸ Contrastingly, **1** and **2** require more reducing potentials (-0.89 and -1.04 V vs SCE, respectively) than either the Bouwman (-0.21 V) or Maverick (-0.32 V) reports, correlating with larger estimated pseudo-first-order rate constants for $\text{CO}_2\text{-RedOx}$ at 298 K. Attempts to coordinate ligands to **1** or **2** have been unsuccessful, implying minimal product inhibition here. Consistently, the highest catalytic rate constant for a Ni(I) complex reported by Jäger is $\sim 1 \times 10^5 \text{ M}^{-1} \text{ s}^{-1}$, and the onset potential for that catalyst is -2.24 V vs SCE.^{7b} Values for k_{obs} are larger for 2^- than the analogous I^- complex, further reinforcing this observation. This conclusion resembles prior reported correlations between $E_{1/2}$ and reaction rate for O_2 reduction electrocatalysts¹⁶ and in H_2 electrocatalysis.¹⁷ One aspect of catalyst design for CO_2RedOx is the balance between reducing power of the reactive species and product inhibition.^{6b}

In our proposed mechanism (Scheme 1), $[\text{Cu}_3\text{EL}]^-$ reacts with CO_2 , affording $[\text{Cu}_3\text{EL}(\text{CO}_2)]^-$, which is short-lived based on our kinetic data. Electron transfer from $[\text{Cu}_3\text{EL}]^-$ to CO_2 is likely rate controlling and not C–C bond formation, as k_{obs} values determined from A_{680} and A_{805} are within error. The cation dependence observed here evokes reports on the influence of redox-innocent cations and proximal hydrogen-bonding interactions in facilitating O_2 and CO_2 bond scission.^{18,19} Indeed, the calculated ΔS^\ddagger values are consistent with an ordered transition state in the rate-controlling step, and

Scheme 1. Proposed Mechanism of CO_2 Activation and Influence of Cation in Stabilizing Intermediates

our activation parameters are comparable to those reported for O_2 activation in the presence of cations and for CO_2 capture.^{18b,c,20} Therefore, an analogous transient in which the cation accelerates electron transfer to CO_2 is likely present here as well. In a similar vein, solvent is reported to tune product distribution for stoichiometric CO_2 reduction by an iron(I) complex;²¹ solvent modulates reaction kinetics without affecting product distribution for $[\text{Cu}_3\text{EL}]^-$.

The order in CO_2 is inconsistent with $\text{CO}_2^{\bullet-}$ dissociation, differing from Jäger's examples and suggesting a more complex mechanism (Scheme 1, vertical arrow).^{7b} Tanaka proposed that one CO_2 molecule first binds to a μ_3 -sulfide in the $[\text{M}_3\text{S}_2]^{2+}$ catalysts, and a second CO_2 then coordinates to a metal center, followed by intramolecular C–C coupling,^{7d} which resembles the mechanisms proposed for CO_2 reduction by Mo(O)SCu carbon monoxide dehydrogenase and CO_2 reduction by a nucleophilic metal nitride.²² However, the chalcogens in **1** and **2** are sterically inaccessible to CO_2 , implicating an alternate structure for the initial CO_2 adduct here. In contrast to other multimetallic CO_2RedOx catalysts, I^- and 2^- are one-electron reductants, necessitating a bis(Cu_3EL) transient or inter-complex electron transfer (Scheme 1). DFT calculations on the Bouwman system propose a CO_2 -bridged dicopper species prior to C–C bond formation.^{15b} A $[(\text{Cu}_3\text{EL})_2(\text{CO}_2)]^{2-}$ transient would be comparable, and we note that approach of two trimetallic cyclophanates is sterically feasible.²³ High $[\text{CO}_2]$ could sequester $[\text{Cu}_3\text{EL}]^-$ as the CO_2 adduct, effectively lowering $[\text{Cu}_3\text{EL}]^-$ and slowing oxalate formation. Such a kinetic condition necessarily accumulates $[\text{Cu}_3\text{EL}(\text{CO}_2)]^-$, which is inconsistent with our data. Reactions at significantly higher $[\text{CO}_2]$ may allow observation of this adduct, and these experiments are part of ongoing investigations. In the final step,

C–C bond formation results from nucleophilic attack by the bound CO₂ on an unactivated CO₂, liberating oxalate and Cu₃EL.

In conclusion, Cu₃EL (E = S, Se) are competent chemical catalysts for CO₂ reduction to oxalate, with **2** exhibiting near-quantitative yield of oxalate using a variety of reductants in the presence of alkali cations. Our results reinforce that counter-cation and solvent can be critical parameters in the reductive activation of small-molecule substrates. Current efforts aim to improve the catalytic rate and energetic cost as well as transition toward other electron sources.

■ ASSOCIATED CONTENT

● Supporting Information

The Supporting Information is available free of charge on the ACS Publications website at DOI: [10.1021/jacs.8b02508](https://doi.org/10.1021/jacs.8b02508).

Synthetic protocols, spectroscopic characterization, stopped-flow UV/visible data for reported compounds and reactions, including Figures S1–S108 and Tables S1–S7 (PDF)

X-ray crystallographic data for [K(THF)₃][Cu₃SL] (CIF)

X-ray crystallographic data for [K(THF)₃][Cu₃SeL] (CIF)

■ AUTHOR INFORMATION

Corresponding Author

*murray@chem.ufl.edu

ORCID

Leslie J. Murray: [0000-0002-1568-958X](https://orcid.org/0000-0002-1568-958X)

Notes

The authors declare no competing financial interest.

■ ACKNOWLEDGMENTS

L.J.M. acknowledges a University of Florida departmental instrumentation award (NSF CHE-1048604), ACS Petroleum Research Fund (ACS-PRF 52704-DNI3), and NSF CHE-1464876. G.N.D. acknowledges a University of Florida, College of Liberal Arts and Sciences Graduate Research Fellowship. K.A.A. acknowledges University of Florida and NSF CHE-0821346 for funding an X-ray equipment purchase.

■ REFERENCES

- (1) Appel, A. M.; Bercaw, J. E.; Bocarsly, A. B.; Dobbek, H.; DuBois, D. L.; Dupuis, M.; Ferry, J. G.; Fujita, E.; Hille, R.; Kenis, P. J. A.; Kerfeld, C. A.; Morris, R. H.; Peden, C. H. F.; Portis, A. R.; Ragsdale, S. W.; Rauchfuss, T. B.; Reek, J. N. H.; Seefeldt, L. C.; Thauer, R. K.; Waldrop, G. L. *Chem. Rev.* **2013**, *113*, 6621–6658.
- (2) Mondal, B.; Song, J.; Neese, F.; Ye, S. *Curr. Opin. Chem. Biol.* **2015**, *25*, 103–109.
- (3) (a) Matson, E. M.; Forrest, W. P.; Fanwick, P. E.; Bart, S. C. *J. Am. Chem. Soc.* **2011**, *133*, 4948–4954. (b) Chen, W.-C.; Shen, J.-S.; Jurca, T.; Peng, C.-J.; Lin, Y.-H.; Wang, Y.-P.; Shih, W.-C.; Yap, G. P. A.; Ong, T.-G. *Angew. Chem., Int. Ed.* **2015**, *54*, 15207–15212. (c) Specklin, D.; Flidel, C.; Gourlaouen, C.; Bruyere, J.-C.; Avilés, T.; Boudon, C.; Ruhlmann, L.; Dagorne, S. *Chem. - Eur. J.* **2017**, *23*, 5509–5519. (d) Zhang, Y.; Hanna, B. S.; Dineen, A.; Williard, P. G.; Bernskoetter, W. H. *Organometallics* **2013**, *32*, 3969–3979. (e) Hanna, B. S.; MacIntosh, A. D.; Ahn, S.; Tyler, B. T.; Palmore, G. T. R.; Williard, P. G.; Bernskoetter, W. H. *Organometallics* **2014**, *33*, 3425–3432. (f) Tate, B. K.; Jordan, A. J.; Bacsá, J.; Sadighi, J. P. *Organometallics* **2017**, *36*, 964–974. (g) Bhattacharyya, K. X.; Akana, J. A.; Laitar, D. S.; Berlin, J. M.; Sadighi, J. P. *Organometallics* **2008**, *27*, 2682–2684.
- (4) (a) Simón-Manso, E.; Kubiak, C. P. *Organometallics* **2005**, *24*, 96–102. (b) Roy, S.; Blane, T.; Lilio, A.; Kubiak, C. P. *Inorg. Chim. Acta* **2011**, *374*, 134–139. (c) Keith, J. A.; Grice, K. A.; Kubiak, C. P.; Carter, E. A. *J. Am. Chem. Soc.* **2013**, *135*, 15823–15829. (d) Clark, M. L.; Grice, K. A.; Moore, C. E.; Rheingold, A. L.; Kubiak, C. P. *Chem. Sci.* **2014**, *5*, 1894–1900. (e) Sampson, M. D.; Kubiak, C. P. *Inorg. Chem.* **2015**, *54*, 6674–6676. (f) Sampson, M. D.; Kubiak, C. P. *J. Am. Chem. Soc.* **2016**, *138*, 1386–1393. (g) Bourrez, M.; Molton, F.; Chardon-Noblat, S.; Deronzier, A. *Angew. Chem., Int. Ed.* **2011**, *50*, 9903–9906. (h) Morris, A. J.; Meyer, G. J.; Fujita, E. *Acc. Chem. Res.* **2009**, *42*, 1983–1994. (i) Sato, S.; Ishitani, O. *Coord. Chem. Rev.* **2015**, *282–283*, 50–59. (j) Wang, T.; Stephan, D. W. *Chem. - Eur. J.* **2014**, *20*, 3036–3039. (k) Wang, T.; Stephan, D. W. *Chem. Commun.* **2014**, *50*, 7007–7010. (l) Theuergarten, E.; Schlösser, J.; Schluns, D.; Freytag, M.; Daniliuc, C. G.; Jones, P. G.; Tamm, M. *Dalton Trans.* **2012**, *41*, 9101–9110. (m) Courtemanche, M.-A.; Légaré, M.-A.; Maron, L.; Fontaine, F.-G. *J. Am. Chem. Soc.* **2013**, *135*, 9326–9329. (n) Sgro, M. J.; Stephan, D. W. *Angew. Chem., Int. Ed.* **2012**, *51*, 11343–11345. (o) Courtemanche, M.-A.; Pulis, A. P.; Rochette, E.; Légaré, M.-A.; Stephan, D. W.; Fontaine, F.-G. *Chem. Commun.* **2015**, *51*, 9797–9800.
- (5) (a) Han, Z.; Kortlever, R.; Chen, H.-Y.; Peters, J. C.; Agapie, T. *ACS Cent. Sci.* **2017**, *3*, 853–859. (b) Li, C. W.; Kanan, M. W. *J. Am. Chem. Soc.* **2012**, *134*, 7231–7234. (c) Min, X.; Kanan, M. W. *J. Am. Chem. Soc.* **2015**, *137*, 4701–4708. (d) Verdaguer-Casadevall, A.; Li, C. W.; Johansson, T. P.; Scott, S. B.; McKeown, J. T.; Kumar, M.; Stephens, I. E. L.; Kanan, M. W.; Chorkendorff, I. *J. Am. Chem. Soc.* **2015**, *137*, 9808–9811. (e) Banerjee, A.; Dick, G. R.; Yoshino, T.; Kanan, M. W. *Nature* **2016**, *531*, 215–219. (f) Feng, X.; Jiang, K.; Fan, S.; Kanan, M. W. *ACS Cent. Sci.* **2016**, *2*, 169–174. (g) Ma, S.; Sadakiyo, M.; Heima, M.; Luo, R.; Haasch, R. T.; Gold, J. I.; Yamauchi, M.; Kenis, P. J. A. *J. Am. Chem. Soc.* **2017**, *139*, 47–50. (h) Dutta, A.; Rahaman, M.; Mohos, M.; Zanetti, A.; Broekmann, P. *ACS Catal.* **2017**, *7*, 5431–5437. (i) Tang, Q.; Lee, Y.; Li, D.-Y.; Choi, W.; Liu, C. W.; Lee, D.; Jiang, D.-E. *J. Am. Chem. Soc.* **2017**, *139*, 9728–9736. (j) Lum, Y.; Yue, B.; Lobaccaro, P.; Bell, A. T.; Ager, J. W. *J. Phys. Chem. C* **2017**, *121*, 14191–14203. (k) Nie, X.; Wang, H.; Janik, M. J.; Chen, Y.; Guo, X.; Song, C. *J. Phys. Chem. C* **2017**, *121*, 13164–13174. (l) Hoang, T. T. H.; Ma, S.; Gold, J. I.; Kenis, P. J. A.; Gewirth, A. A. *ACS Catal.* **2017**, *7*, 3313–3321. (m) Huang, Y.; Handoko, A. D.; Hirunsit, P.; Yeo, B. S. *ACS Catal.* **2017**, *7*, 1749–1756. (n) Xiao, H.; Cheng, T.; Goddard, W. A. *J. Am. Chem. Soc.* **2017**, *139*, 130–136. (o) Yang, X.; Fugate, E. A.; Mueanngrn, Y.; Baker, L. R. *ACS Catal.* **2017**, *7*, 177–180.
- (6) (a) Gennaro, A.; Isse, A. A.; Severin, M.-G.; Vianello, E.; Bhugun, I.; Savéant, J.-M. *J. Chem. Soc., Faraday Trans.* **1996**, *92*, 3963–3968. (b) Costentin, C.; Robert, M.; Savéant, J.-M. *Chem. Soc. Rev.* **2013**, *42*, 2423–2436.
- (7) (a) Angamuthu, R.; Byers, P.; Lutz, M.; Spek, A. L.; Bouwman, E. *Science* **2010**, *327*, 313–315. (b) Rudolph, M.; Dautz, S.; Jäger, E.-G. *J. Am. Chem. Soc.* **2000**, *122*, 10821–10830. (c) Becker, J. Y.; Vainas, B.; Eger, R.; Kaufman, L. *J. Chem. Soc., Chem. Commun.* **1985**, 1471–1472. (d) Tanaka, K.; Kushi, Y.; Tsuge, K.; Toyohara, K.; Nishioka, T.; Isobe, K. *Inorg. Chem.* **1998**, *37*, 120–126. (e) Pulliam, C. R.; Thoden, J. B.; Stacy, A. M.; Spencer, B.; Englert, M. H.; Dahl, L. F. *J. Am. Chem. Soc.* **1991**, *113*, 7398–7410. (f) Nishioka, T.; Isobe, K. *Chem. Lett.* **1994**, *23*, 1661–1664. (g) Venturelli, A.; Rauchfuss, T. B. *J. Am. Chem. Soc.* **1994**, *116*, 4824–4831.
- (8) Horn, B.; Limberg, C.; Herwig, C.; Braun, B. *Chem. Commun.* **2013**, *49*, 10923–10925.
- (9) Pokharel, U. R.; Fronczek, F. R.; Maverick, A. W. *Nat. Commun.* **2014**, *5*, 6883.
- (10) (a) Burgess, S. A.; Appel, A. M.; Linehan, J. C.; Wiedner, E. S. *Angew. Chem., Int. Ed.* **2017**, *56*, 15002–15005. (b) Singh, M. R.; Kwon, Y.; Lum, Y.; Ager, J. W.; Bell, A. T. *J. Am. Chem. Soc.* **2016**, *138*, 13006–13012.

- (11) Castillo, M.; Metta-Magaña, A. J.; Fortier, S. *New J. Chem.* **2016**, 40, 1923–1926.
- (12) Di Francesco, G. N.; Gaillard, A.; Ghiviriga, I.; Abboud, K. A.; Murray, L. J. *Inorg. Chem.* **2014**, 53, 4647–4654.
- (13) Cook, B. J.; Di Francesco, G. N.; Ferreira, R. B.; Lukens, J. T.; Silberstein, K. E.; Keegan, B. C.; Catalano, V. J.; Lancaster, K. M.; Shearer, J.; Murray, L. J., Chalcogen Impact on Covalency within Molecular $[\text{Cu}_3(\mu_3\text{-E})]^{3+}$ Clusters (E = O, S, Se): A Synthetic, Spectroscopic, and Computational Study. Manuscript submitted, 2018.
- (14) MacDonald, M. R.; Bates, J. E.; Ziller, J. W.; Furche, F.; Evans, W. J. *J. Am. Chem. Soc.* **2013**, 135, 9857–9868.
- (15) (a) Kefalidis, C. E.; Stasch, A.; Jones, C.; Maron, L. *Chem. Commun.* **2014**, 50, 12318–12321. (b) Lan, J.; Liao, T.; Zhang, T.; Chung, L. W. *Inorg. Chem.* **2017**, 56, 6809–6819. (c) Castro, L.; Lam, O. P.; Bart, S. C.; Meyer, K.; Maron, L. *Organometallics* **2010**, 29, 5504–5510.
- (16) (a) Wasylenko, D. J.; Rodríguez, C.; Pegis, M. L.; Mayer, J. M. *J. Am. Chem. Soc.* **2014**, 136, 12544–12547. (b) Pegis, M. L.; Wise, C. F.; Martin, D. J.; Mayer, J. M. *Chem. Rev.* **2018**, 118, 2340–2391. (c) Pegis, M. L.; Wise, C. F.; Koronkiewicz, B.; Mayer, J. M. *J. Am. Chem. Soc.* **2017**, 139, 11000–11003. (d) Pegis, M. L.; McKeown, B. A.; Kumar, N.; Lang, K.; Wasylenko, D. J.; Zhang, X. P.; Raugei, S.; Mayer, J. M. *ACS Cent. Sci.* **2016**, 2, 850–856.
- (17) (a) Artero, V.; Savéant, J.-M. *Energy Environ. Sci.* **2014**, 7, 3808–3814. (b) Artero, V.; Berggren, G.; Atta, M.; Caserta, G.; Roy, S.; Pecqueur, L.; Fontecave, M. *Acc. Chem. Res.* **2015**, 48, 2380–2387. (c) Canaguier, S.; Fontecave, M.; Artero, V. *Eur. J. Inorg. Chem.* **2011**, 2011, 1094–1099. (d) Fourmond, V.; Jacques, P.-A.; Fontecave, M.; Artero, V. *Inorg. Chem.* **2010**, 49, 10338–10347. (e) Le Goff, A.; Artero, V.; Jousselme, B.; Tran, P. D.; Guillet, N.; Métaillé, R.; Fihri, A.; Palacin, S.; Fontecave, M. *Science* **2009**, 326, 1384–1387. (f) Roy, S.; Bacchi, M.; Berggren, G.; Artero, V. *ChemSusChem* **2015**, 8, 3632–3638.
- (18) (a) Bae, S. H.; Lee, Y.-M.; Fukuzumi, S.; Nam, W. *Angew. Chem., Int. Ed.* **2017**, 56, 801–805. (b) Bang, S.; Lee, Y.-M.; Hong, S.; Cho, K.-B.; Nishida, Y.; Seo, M. S.; Sarangi, R.; Fukuzumi, S.; Nam, W. *Nat. Chem.* **2014**, 6, 934–940. (c) Hong, S.; Lee, Y.-M.; Sankaralingam, M.; Vardhaman, A. K.; Park, Y. J.; Cho, K.-B.; Ogura, T.; Sarangi, R.; Fukuzumi, S.; Nam, W. *J. Am. Chem. Soc.* **2016**, 138, 8523–8532. (d) Lee, Y.-M.; Bang, S.; Kim, Y. M.; Cho, J.; Hong, S.; Nomura, T.; Ogura, T.; Troppner, O.; Ivanovic-Burmazovic, I.; Sarangi, R.; Fukuzumi, S.; Nam, W. *Chem. Sci.* **2013**, 4, 3917–3923. (e) Lee, Y.-M.; Bang, S.; Yoon, H.; Bae, S. H.; Hong, S.; Cho, K.-B.; Sarangi, R.; Fukuzumi, S.; Nam, W. *Chem. - Eur. J.* **2015**, 21, 10676–10680. (f) Yoon, H.; Lee, Y.-M.; Wu, X.; Cho, K.-B.; Sarangi, R.; Nam, W.; Fukuzumi, S. *J. Am. Chem. Soc.* **2013**, 135, 9186–9194. (g) Fachinetti, G.; Floriani, C.; Zanazzi, P. F. *J. Am. Chem. Soc.* **1978**, 100, 7405–7407. (h) Gambarotta, S.; Arena, F.; Floriani, C.; Zanazzi, P. F. *J. Am. Chem. Soc.* **1982**, 104, 5082–5092.
- (19) (a) Reath, A. H.; Ziller, J. W.; Tsay, C.; Ryan, A. J.; Yang, J. Y. *Inorg. Chem.* **2017**, 56, 3713–3718. (b) Bernskoetter, W. H.; Hazari, N. *Acc. Chem. Res.* **2017**, 50, 1049–1058.
- (20) Huang, D.; Makhlynets, O. V.; Tan, L. L.; Lee, S. C.; Rybak-Akimova, E. V.; Holm, R. H. *Proc. Natl. Acad. Sci. U. S. A.* **2011**, 108, 1222–1227.
- (21) Saouma, C. T.; Lu, C. C.; Day, M. W.; Peters, J. C. *Chem. Sci.* **2013**, 4, 4042–4051.
- (22) (a) Pelzmann, A.; Mickoleit, F.; Meyer, O. *JBIC, J. Biol. Inorg. Chem.* **2014**, 19, 1399–1414. (b) Stein, B. W.; Kirk, M. L. *Chem. Commun.* **2014**, 50, 1104–1106. (c) Gourlay, C.; Nielsen, D. J.; White, J. M.; Knottenbelt, S. Z.; Kirk, M. L.; Young, C. G. *J. Am. Chem. Soc.* **2006**, 128, 2164–2165. (d) Silvia, J. S.; Cummins, C. C. *J. Am. Chem. Soc.* **2010**, 132, 2169–2171.
- (23) Lee, Y.; Sloane, F. T.; Blondin, G.; Abboud, K. A.; García-Serres, R.; Murray, L. J. *Angew. Chem., Int. Ed.* **2015**, 54, 1499–1503.
- (24) Solvent influences only reaction rate and not product distribution.
- (25) Cu_3SL decomposes to afford K_3L in the presence of large excesses of KC_8 for extended periods (Figure S57). Similar decomposition is not observed for Cu_3SeL under these conditions (Figure S107–S108).